THE JOURNAL OF BIOLOGICAL CHEMISTRY VOL. 285, NO. 38, pp. 29662–29670, September 17, 2010

Ataxia Telangiectasia Mutated (ATM)-mediated DNA Damage Response in Oxidative Stress-induced Vascular Endothelial Cell Senescence*[S]

Received for publication, March 24, 2010, and in revised form, July 15, 2010 Published, JBC Papers in Press, July 16, 2010, DOI 10.1074/jbc.M110.125138

Hong Zhan[‡1], **Toru Suzuki**[‡§1,2], **Kenichi Aizawa**[‡§1], **Kiyoshi Miyagawa**[¶], **and Ryozo Nagai**[‡3]

From the Departments of [‡]*Cardiovascular Medicine,* [§]*Ubiquitous Preventive Medicine, and* [¶]*Radiation Biology, Graduate School of Medicine, The University of Tokyo, 7-3-1 Hongo, Bunkyo, Tokyo 113-8655, Japan*

Oxidative stress regulates dysfunction and senescence of vascular endothelial cells. The DNA damage response and its main signaling pathway involving ataxia telangiectasia mutated (ATM) have been implicated in playing a central role in mediating the actions of oxidative stress; however, the role of the ATM signaling pathway in vascular pathogenesis has largely remained unclear. Here, we identify ATM to regulate oxidative stress-induced endothelial cell dysfunction and premature senescence. Oxidative stress induced senescence in endothelial cells through activation/phosphorylation of ATM by way of an Akt/p53/p21-mediated pathway. These actions were abrogated in cells in which ATM was knocked down by RNA interference or inhibited by specific inhibitory compounds. Furthermore, the *in vivo* significance of this regulatory pathway was confirmed using ATM knock-out mice in which induction of senescent endothelial cells in the aorta in a diabetic mouse model of endothelial dysfunction and senescence was attenuated in contrast to pathological changes seen in wild-type mice. Collectively, our results show that ATM through an ATM/Akt/p53/p21-dependent signaling pathway mediates an instructive role in oxidative stress-induced endothelial dysfunction and premature senescence.

The DNA damage response is activated in response to stimuli ranging from oxidative stress, oncogenic stress to ionizing radiation to determine which cells remain viable after cytopathogenic insult. Recent reports suggest that the DNA damage response in addition to its classical role in regulating the cell cycle checkpoint in cancer to also play a major regulatory role in nononcogenic fields such as in aging/senescence (1–3). One field in which the DNA damage response has remained poorly addressed is the cardiovasculature.

Aging is known to be a major cardiovascular risk factor (4). Premature senescence in endothelial cells is induced by proatherogenic and proinflammatory factors such as hydrogen peroxide (H_2O_2), oxidized LDL or TNF-α by telomeric inactivation through an Akt-dependent mechanism (5, 6). Because regulation of aging/senescence of the vasculature, notably through the endothelial cell, contributes to mechanisms of arteriosclerosis and other age-related cardiovascular diseases (7), we questioned whether the DNA damage response might play a role in regulation of endothelial regulation of aging/senescence. For this, we focused on the role of ataxia telangiectasia mutated (ATM),[4] which is the central effector molecule in the DNA damage response pathway.

ATM belongs to the phosphoinositide 3-kinase (PI3-kinase)-related protein kinase (PIKK) family which has been identified as the product mutated or inactivated in ataxia telangiectasia (A-T) patients. The DNA damage response and its main signaling pathway involving ATM have been implicated in playing a central role in mediating the actions of oxidative stress (8–10). However, the role of the ATM signaling pathway in vascular pathogenesis has remained unclear. Further, pathogenic mechanisms of the vascular pathologies associated with mutated ATM (telangiectasia, premature coronary artery disease) remain obscure.

In the present study, we examined the effects of ATM-mediated oxidative stress-induced senescence in vascular pathologies through actions on endothelial cells. Our results show that ATM through an ATM/Akt/p53/p21-dependent signaling pathway mediates an instructive role in oxidative stress-induced endothelial dysfunction and premature senescence.

EXPERIMENTAL PROCEDURES

Cell Culture—Human umbilical vein endothelial cells (HUVECs) were purchased from Sanko Junyaku (Tokyo, Japan) and maintained with endothelial cell basal medium-2 containing EGM-2 supplement as purchased from Cambrex Bio Science (Rockland, MD) in humidified air with 5% CO_2 at 37 °C. All experiments were performed between passages 4 and 6.

Western Blot Analysis and Antibodies—HUVECs (3×10^5 cells/well) were treated with 100 μM H_2O_2 in the absence or presence of *N*-acetyl-L-cysteine (NAC) (Sigma-Aldrich), caffeine (Wako, Osaka, Japan), or KU-55933 (Calbiochem). Cells were washed with cold phosphate-buffered saline (PBS) and

* This work was supported by grants-in-aid for scientific research (T. S., K. A., and R. N.) from the Ministry of Education, Culture, Sports, Science, and Technology, Japan.

[S] The on-line version of this article (available at http://www.jbc.org) contains supplemental Experimental Procedures and Figs. 1–7.

[1] These authors contributed equally to this work.

[2] To whom correspondence may be addressed: Dept. of Cardiovascular Medicine, Graduate School of Medicine, The University of Tokyo, 7-3-1 Hongo, Bunkyo, Tokyo 113-8655, Japan. Tel.: 81-3-5800-9846; Fax: 81-3-5800-9847; E-mail: torusuzu-tky@umin.ac.jp.

[3] To whom correspondence may be addressed. Tel.: 81-3-5800-6526; Fax: 81-3-3815-2087; E-mail: nagai-tky@umin.ac.jp.

[4] The abbreviations used are: ATM, ataxia telangiectasia mutated; A-T, ataxia telangiectasia; BisTris, bis(2-hydroxyethyl)iminotris(hydroxymethyl)methane; DSB, DNA double-strand break; HUVEC, human umbilical vein endothelial cell; NAC, *N*-acetyl-L-cysteine; SA-β-gal, senescence-associated β-galactosidase; STZ, streptozotocin.

lysed with 2× NuPAGE LDS sample buffer (Invitrogen) supplemented with 1 mM sodium orthovanadate (Sigma-Aldrich) and 1 mM sodium fluoride (Wako). Lysates were then boiled for 10 min and centrifuged for 2 min at 4 °C. Equal amounts of protein were separated by NuPAGE 3–8% Tris acetate mini gel electrophoresis or NuPAGE 10% BisTris gel (Invitrogen) and then transferred onto a polyvinylidine difluoride (PVDF) membrane (Invitrogen). Membranes were blocked with 5% skim milk in PBS at room temperature for 1 h and then subsequently probed with primary antibodies at a predetermined optimal concentration for 2–4 h at room temperature or overnight at 4 °C. After rinsing with TBS containing 0.1% Triton X-100 (TBS-T), membranes were incubated with appropriate horseradish peroxidase-conjugated anti-rabbit (Cell Signaling Technology) or anti-mouse IgG (GE Healthcare) for 1 h at room temperature. After three washes with TBS-T, immunoblots were detected using the ECL Plus Western blotting Detection System (GE Healthcare) and exposed to x-ray film (Fuji medical x-ray film, Tokyo, Japan). Anti-phospho-ATM (Ser^{1981}) antibody was purchased from Millipore; anti-ATM (2C1) and anti-p53 (DO-1) antibodies were from Santa Cruz Biotechnology (Santa Cruz, CA); and anti-phospho-p53 (Ser^{15}), anti-phospho-Akt (Ser^{473}), and anti-Akt antibodies were from Cell Signaling Technology. Anti-GAPDH antibody (Life Technologies) was used as a loading control. Purified mouse anti-p21 antibody was obtained from BD Pharmingen. See also supplemental Experimental Procedures.

Immunofluorescence Microscopy—Cells were grown on coverslips at a density of 1×10^5 per slide. After treatment with 100 μM H_2O_2 for 1 h, cells were fixed in 3% paraformaldehyde in PBS for 10 min. Chamber slides were washed three times with PBS and then permeabilized with 0.25% Triton X-100 in PBS for 10 min. After washing twice with PBS and blocking for 5 min with 0.1% gelatin, slides were incubated with primary antibody (1:100) in 0.1% gelatin in PBS for 1 h in a humidified chamber at 37 °C. Cells were blocked three times with 0.1% gelatin, and then samples were incubated with secondary antibody using Alexa Fluor 488 green or Alexa Fluor 635 red (Life Technologies) in 0.1% gelatin in PBS for 1 h in a humidified chamber at 37 °C. Antibodies used for immunofluorescence were ATM-Ser^{1981}, ATM, p53-Ser^{15}, p53, p21, and 53BP1 (Cell Signaling Technology). Nuclei were stained with Hoechst 33258 and mounted with DakoCytomation Fluorescent Mounting Medium (Dako Japan, Kyoto, Japan) and then visualized with a Carl Zeiss LSM510 confocal microscope (Carl Zeiss, Jena, Germany).

Senescence-induced by Oxidative Stress and Senescence-associated β-Galactosidase (SA-β-gal) Staining—Methods for inducing premature senescence by H_2O_2 (Wako) have been described previously (11). Briefly, HUVECs (3×10^5 cells/well) were grown in 30-mm collagen-coated dishes to 80% confluence. Cells were pretreated for 3 days with vehicle, NAC (0.1, 2, and 10 mM), caffeine (0.1, 2, and 5 mM), or KU-55933 (0.5, 5, and 10 μM). After washing three times with endothelial cell basal medium-2 and treating for 1 h with 100 μM H_2O_2, cells were trypsinized, reseeded at a density of 5×10^4 in 30-mm dishes, and cultured with endothelial cell basal medium-2 containing compound for 10 days. Cells were then washed in PBS and fixed for 5 min at room temperature in 2% formaldehyde/0.2% glutaraldehyde, washed, and then incubated at 37 °C for 12 h (without CO_2) with fresh SA-β-gal stain solution which contained 1 mg/ml 5-bromo-4-chloro-3-indolyl-β-D-galactoside (X-Gal), 40 mM citric acid/sodium phosphate, pH 6.0, 5 mM potassium ferrocyanide, 5 mM potassium ferricyanide, 150 mM sodium chloride, and 2 mM magnesium chloride. Senescent cells were identified as blue-stained cells by phase contrast microscopy, and a total of 1,000 cells were counted in 20 random fields to determine the percentage of SA-β-gal-positive cells.

RNA Interference—Small interference RNA (siRNA) constructs were obtained as siGENOME SMARTpool reagent from Dharmacon. See also supplemental Experimental Procedures. A siRNA pool specific for ATM (siGENOME SMARTpool Human ATM, M-003201020005) and control siRNA (siGENOME nontargeting siRNA pool, D-0012061320) were used. HUVECs (3×10^5 cells/well) were grown to 80% confluence in 6-well culture dishes. Transient transfections of 10, 50, and 100 pmol of ATM siRNA or nontarget siRNA were performed by a liposome-mediated method using Lipofectamine 2000 according to the manufacturer's instructions (Invitrogen). The indicated amounts of siRNA and 5 μl of Lipofectamine 2000 were, respectively, diluted in 0.25 ml of Opti-MEM without serum. After incubation for 5 min, diluted siRNA and Lipofectamine 2000 were combined, and the mixture was incubated for 20 min at room temperature to allow the DNA·Lipofectamine 2000 complexes to form. 0.5 ml of complex was added to each well. After 5 h of transfection, the medium with complexes was removed, and endothelial cell basal medium-2 supplemented with EGM-2 was added. At 72 h following transient transfection, total RNA was extracted and submitted to reverse transcription-PCR (RT-PCR) experiments using oligonucleotide primers specific to ATM and 18 S rRNA. In ATM knock-down cells, the levels of total ATM, phospho-p53 (Ser^{15}), phospho-Akt (Ser^{473}), total Akt, or GAPDH proteins were analyzed by Western blotting, or SA-β-gal activity was measured.

RNA Extraction and Quantitative RT-PCR—Total RNA from HUVECs (3×10^5 cells/well) was extracted by the RNeasy Mini kit (Qiagen) according to the manufacturer's instructions. RNA concentration and purity were determined on a spectrophotometer (Ultrospec 3000; GE Healthcare) by calculating the ratio of optical density at 260 nm to 280 nm. One microgram of total RNA sample was used to generate first-strand complementary DNA by using powerscript reverse transcriptase (Clontech) according to the manufacturer's recommended procedures. PCR was then performed for ATM from the same complementary DNA samples using HotStarTaq (Qiagen), 10× PCR buffer, and 2.5 mM dNTP mix. The forward primer 5′-GATGTTGTTGTCCCTACTATGG-3′ and the reverse primer 5′-GCTACACTGCGCGTATAAGCC-3′ corresponded to human ATM. 18 S rRNA (Life Technologies) was used as an internal control. Amplification was initiated by 15 min of denaturation at 95 °C for 1 cycle followed by 30 cycles at 95 °C for 30 s, 57 °C for 30 s, and 72 °C for 40 s. After the last cycle of amplification, samples were incubated at 72 °C for 10 min in a GeneAmp™ PCR system (Applied Biosystems). PCR products, a 589-bp ATM fragment and a 350-bp 18 S fragment, were then visualized by UV

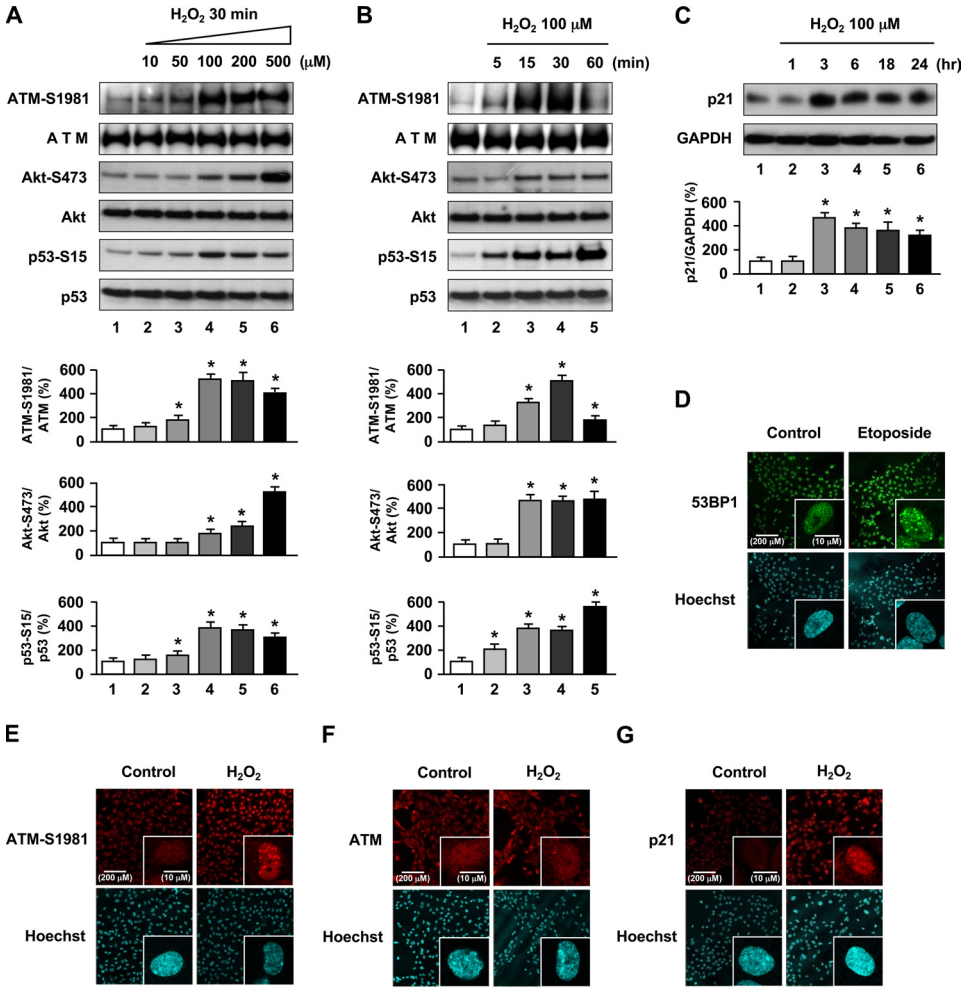

FIGURE 1. **Oxidative stress induces ATM-S1981, Akt-S473, p53-S15 phosphorylation and up-regulation of p21 expression in HUVECs.** *A*, cells were incubated with H_2O_2 for 30 min at the indicated concentrations. *B* and *C*, HUVECs were incubated in 100 μM H_2O_2 for the indicated times. Cells were lysed and subjected to Western blot analyses with the indicated antibodies. GAPDH was used as loading control. Values are mean ± S.E. (*error bars*) ($n = 3$). *, $p < 0.05$ *versus* cells incubated without H_2O_2 treatment. Representative blots are shown in the *upper panels* whereas corresponding quantitation is shown in the *lower panels*. *D–F*, immunofluorescence for 53BP1, phosphorylated ATM-S1981, and total ATM is shown. Cells were exposed to 10 μM etoposide or 100 μM H_2O_2 for 1 h and then immunostained for 53BP1 (*D*), ATM-S1981 (*E*) and total ATM (*F*). Cells incubated without etoposide or H_2O_2 were used as controls. *G*, cells were exposed to 100 μM H_2O_2 for 3 h and then immunostained for p21. Hoechst 33258 was used as nuclear stain (*blue*). Original magnification, ×200 and ×630. *Scale bars*, 200 μm and 10 μm, respectively. Treatment with etoposide and immunofluorescence for 53BP1 (labeled by green fluorescence) was used for a positive control. Expression of phosphorylated ATM-S1981) and p21 labeled by red fluorescence in HUVECs and foci formation was significantly increased after H_2O_2 treatment. Additional views of the photographs are shown in supplemental Fig. 1.

illumination after electrophoresis by 2% agarose gels containing 0.5 μg/ml ethidium bromide.

Animal Experiments—ATM knock-out mice (129S6/SvEvTac-*Atm*^{tm1Awb}/J) were obtained from Jackson Laboratories. All generations were from matings of heterozygous parents. The following sequence, as recommended by Jackson Laboratories, was used for genotyping: oIMR640, 5′-GCTGCCATACTTGATCAATG-3′; oIMR641, 5′-TCCGAATTTGCAGGAGTG-3′; oIMR0013, 5′-CTTGGGTGGAGAGGCTATTC-3; and oIMR0014, 5′-AGGTGAGATGACAGGAGATC-3′. Age-matched 10-week-old SPF male ATM wild-type ($^{+/+}$), heterozygote ($^{+/-}$), and homozygote ($^{-/-}$) mice ($n = 6$, respectively, weighing ~15–25 g) were used. Hyperglycemia was induced by a single intraperitoneal injection of streptozotocin (STZ) (180 mg/kg; Sigma-Aldrich). Tail blood glucose was assayed 3 days after injection using glucose test strips (Roche Applied Science). All diabetic animals had blood glucose values >300 mg/dl. Mice were housed under constant temperature (23 ± 1 °C) with a 12-h light and 12-h dark cycle for 10 days with free access to water and chow and were killed by cervical dislocation. The aorta was removed after systemic perfusion with PBS for histological examination. The aorta was fixed for 30 min at room temperature in 2% formaldehyde/0.2% glutaraldehyde, washed, incubated at 37 °C for 24 h (without CO_2) with fresh SA-β-gal stain solution, and then embedded in OTC compound before freezing in liquid nitrogen. The samples were stored at −80 °C until sample slides were prepared. The proportion of SA-β-gal-positive cells were analyzed by Scion Image software. Serial cross-sections (10 μm) were obtained from each sample and stained with kernechtrot staining solution (Muto, Tokyo, Japan) or prepared for immunohistochemistry. All experimental protocols complied with the guidelines for animal experiments of the University of Tokyo.

Tissue Protein Extraction—Thoracic aorta of ATM knock-out mice (ATM$^{+/+}$, ATM$^{+/-}$, ATM$^{-/-}$ mice) were dissected out of their thoracic aortas and snap frozen in liquid nitrogen. After thawing on ice, the thoracic aortas were homogenized mechanically at 25 Hz for 25 s five times on ice in 150 μl of RIPA buffer (0.1% SDS, 0.5% Nonidet P-40, 0.1% sodium deoxycholate, 150 mM NaCl, 50 mM Tris-HCl, pH 7.9, and 1× EDTA-free complete proteinase inhibitor (Roche Applied Science)). Samples were lysed gently on ice for 30–60 min, and cellular debris was removed by centrifugation. Protein was then quantified using the BCA protein assay kit (Thermo). A 30-μg aliquot of total protein was analyzed for ATM protein by Western blot analysis. Anti-GAPDH antibody was used as a loading control.

Immunohistochemistry—Immunostaining was performed using the Envision kit (Dako Japan). Frozen sections, 10 μm thick, were fixed in acetone at 4 °C, washed in TBS, and then blocked by 0.03% hydrogen peroxidase in methanol. After blocking nonspecific antibody-binding sites, the sections were incubated for 1 h with antibodies against von Willebrand factor (1:1,000; Abcam), p21 and p16 (Santa Cruz Biotechnology) as the primary antibody and then for 1 h with the peroxidase-

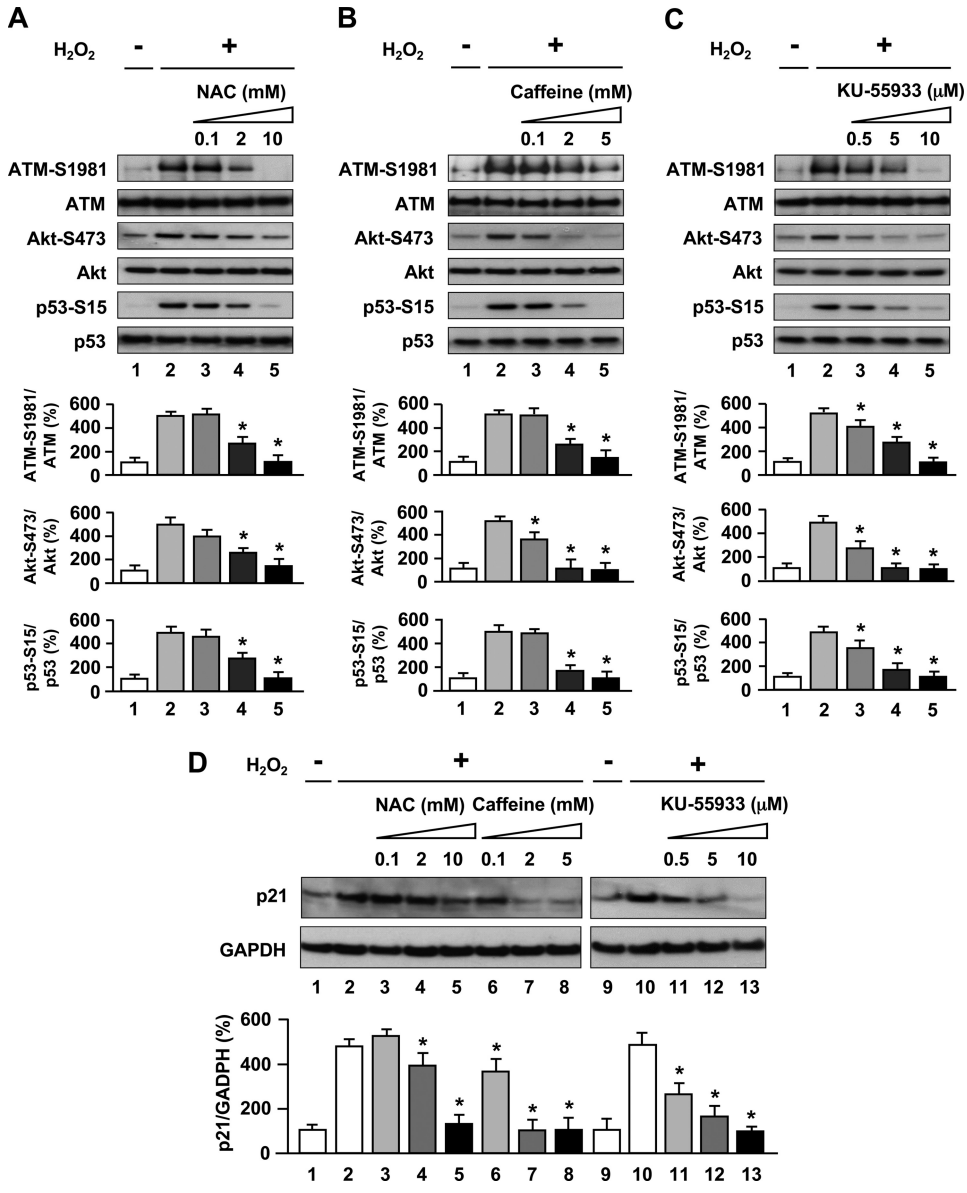

FIGURE 2. **Oxidative stress-induced Akt and p53 phosphorylation and up-regulation of p21 expression are dependent on ATM kinase.** *A–C*, antioxidant and ATM inhibitors blocked phosphorylation of ATM-S1981, Akt-S473, and p53-S15 as stimulated by H_2O_2 exposure. Cells were treated with 100 μM H_2O_2 for 30 min in the absence or presence of NAC (*A*) or caffeine (*B*), or KU-55933 (*C*), and whole cell lysates were subjected to Western blot analyses using the indicated antibodies. *D*, antioxidant and ATM inhibitors down-regulated p21 induction as stimulated by H_2O_2 exposure. Cells were pretreated with NAC, caffeine, or KU-55933 and then 100 μM H_2O_2 for 3 h. Whole cell lysates were subjected to Western blot analyses using p21 antibody. GAPDH was used as loading control. Values are mean ± S.E. (*error bars*) ($n = 3$). *, $p < 0.05$ *versus* cells incubated with H_2O_2. Representative blots are shown in the *upper panels* whereas corresponding quantitation is shown in the *lower panels*.

vation and expression of ATM in cultured HUVECs treated with H_2O_2 as an inducing agent of oxidative stress. HUVECs exposed to H_2O_2 showed increased ATM phosphorylation at Ser^{1981} (ATM-S1981) (Fig. 1, *A* and *B*), which releases it from an inhibitory homodimer structure leading to its activation and recruitment to sites of DNA double-strand breaks (DSBs) (12–14). We next investigated factors involved in the ATM signaling pathway. Because ATM mediates activation of Akt in response to insulin or ionizing radiation which then in turn results in radiosensitivity or resistance to insulin in cell lines derived from A-T patients and ATM knock-out mice (15), we first investigated the activation of Akt in response to oxidative stress. Akt phosphorylation at Ser^{473} (Akt-S473) was increased in H_2O_2-treated HUVECs (Fig. 1, *A* and *B*). We then investigated involvement of p53, a downstream signaling molecule of ATM (10) and Akt (6), which showed phosphorylation at Ser^{15} (p53-S15) after exposure to H_2O_2 (Fig. 1, *A* and *B*). Furthermore, p21, a downstream target of p53, was increased in H_2O_2-treated HUVECs (Fig. 1*C*). Our results indicate that oxidative stress phosphorylates ATM and its involved genes, Akt and p53, with subsequent up-regulation of p21 expression. Thus, the phosphorylation of ATM, Akt, and p53 and up-regulation of p21 expression mediate actions of oxidative stress in endothelial cells.

Although ATM is predominantly present in the nucleus, a variable amount (<10%) has been reported in the cytoplasm, especially in neuronal cells. The major known role of nuclear ATM is to participate in the response to DSBs for DNA repair and cell cycle checkpoint activation (16). In response to agents that induce DSBs, ATM has been found to relocalize to the sites of breaks and in doing so forms large nuclear foci (17). To determine whether oxidative stress-induced ATM forms foci, immunofluorescence analyses for phospho-ATM (Ser^{1981}), total ATM, and p21 were performed. Increased fluorescence and foci formation were seen in response to H_2O_2 for phosphorylated ATM (Fig. 1*E* and supplemental Fig. 1*B*) and increased p21 (Fig. 1*G* and supplemental Fig. 1*D*) under conditions in which 53BP1 formed nuclear foci in response to etoposide as reported

labeled polymer. Finally, sections were incubated with diaminobenzidine tetrahydrochloride (Dako Japan), and the nuclei were counterstained with hematoxylin.

Statistical Analysis—All values are expressed as mean ± S.E. Differences between two groups were analyzed using the two-tailed Student's *t* test. Threshold of significance was taken as $p < 0.05$.

RESULTS

ATM Is Activated by Oxidative Stress in Vascular Endothelial Cells—To investigate the involvement of ATM in mediating oxidative stress in the vasculature, we first examined the acti-

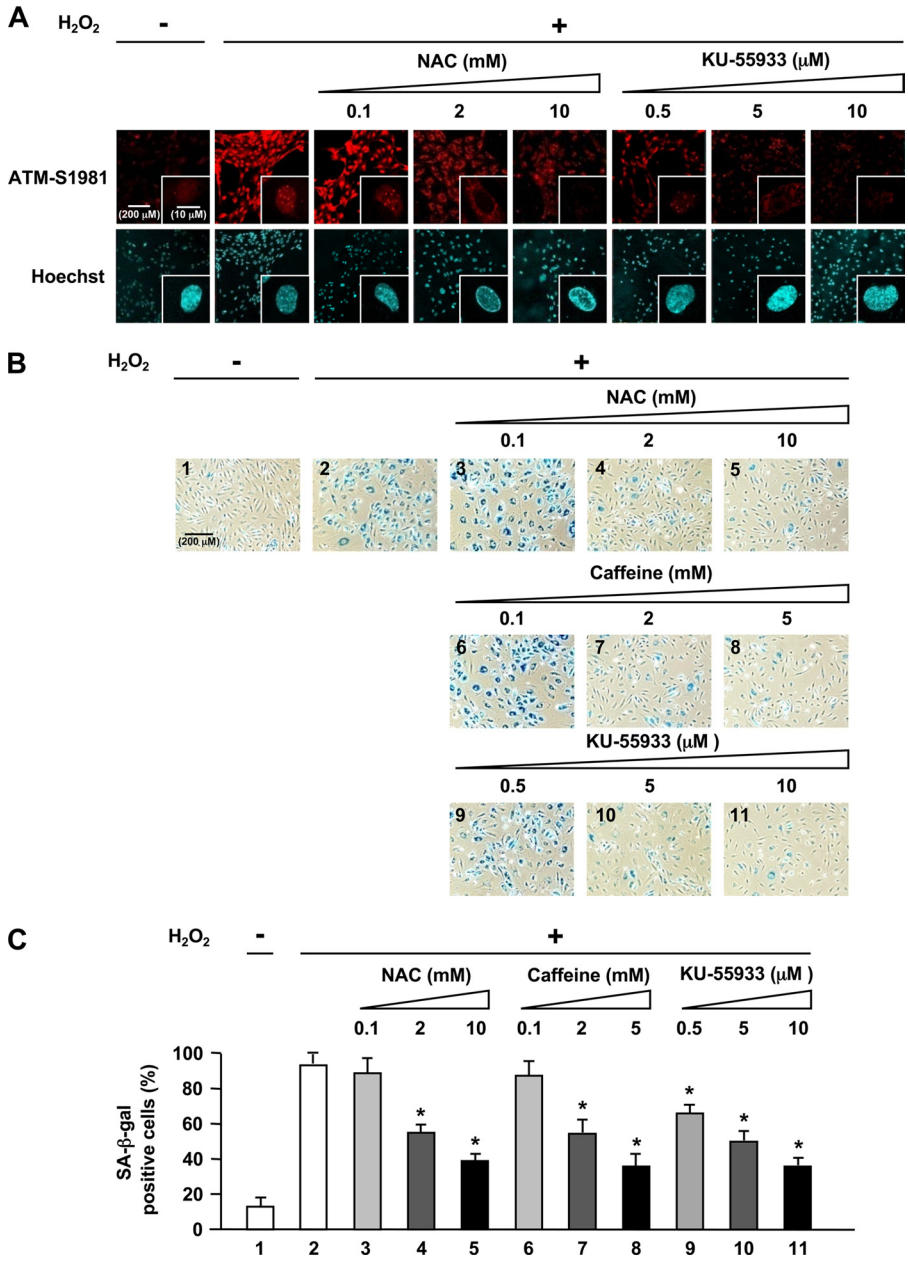

FIGURE 3. **Oxidative stress-induced endothelial cell senescence involves activation of ATM kinase.** *A*, immunofluorescence analysis of the effects of antioxidant (NAC) and ATM inhibitor (KU-55933) on phosphorylated ATM. Cells were treated with NAC or KU-55933 followed by 100 μM H_2O_2 for 1 h and then immunostained for phosphorylated ATM-S1981. Hoechst 33258 was used as nuclear stain (*blue*). Original magnification, ×200 and ×630. Higher magnification of the representative cells in *A* is shown in supplemental Fig. 2. *Scale bar*, 200 μm and 10 μm, respectively. NAC or KU-55933 greatly reduced phosphorylated ATM nuclear fluorescence and foci formation. *B*, effects of NAC, caffeine, or KU-55933 on premature senescent phenotype induced by H_2O_2 as shown by SA-β-gal staining. *C*, quantification of percentage of SA-β-gal-positive cells in *B*. Values are mean ± S.E. (*error bars*) ($n = 3$). *, $p < 0.05$ *versus* cells incubated with H_2O_2. Original magnification, ×100. *Scale bar*, 200 μm. Pretreatment with NAC, caffeine, or KU-55933 resulted in significant reduction of senescent (SA-β-gal-positive) cells compared with those exposed to H_2O_2 alone.

(Fig. 1*D* and supplemental Fig. 1*A*) (18). Total ATM, in contrast, remained diffusely localized throughout the nucleus, and foci formation was not observed in H_2O_2-treated HUVECs (Fig. 1*F* and supplemental Fig. 1*C*). Activated (phosphorylated) ATM localized to foci, which suggests that it might be recruited to sites of DNA damage caused by oxidative stress (17, 18). However, the authors note that the antibody used (ATM-S1981) is known to also recognize a nonspecific protein, which makes conclusions based on experiments using this antibody inconclusive. We further investigated expression of 53BP1 and γ-H2AX as markers of DSB formation in response to H_2O_2 by immunostaining. In the H_2O_2-treated cells, both 53BP1 and γ-H2AX formed nuclear foci (supplemental Fig. 3), which further supports that ATM is activated in response to DSB formation induced by H_2O_2.

Activation of the ATM-dependent DNA Damage Signaling Pathway Contributes to Endothelial Cell Senescence—To better confirm actions of activation of ATM by oxidative stress in endothelial cells, effects of inhibitors of oxidative stress and of ATM were tested. HUVECs were pretreated with NAC, an antioxidant and glutathione precursor that alters the redox state of cells (19), to assess whether ATM phosphorylation was caused by H_2O_2-induced redox imbalance. Western blot analysis showed that pretreatment of endothelial cells with NAC blocked the stimulatory effects of H_2O_2 on the expression of ATM-S1981, Akt-S473, p53-S15 (*lanes 3–5* in Fig. 2*A*) and p21 (*lanes 3–5* in Fig. 2*D*). These results suggest a direct role of H_2O_2 in ATM phosphorylation and activation of involved genes. We further employed two inhibitors, caffeine and KU-55933, to inhibit ATM kinase activity to examine whether Akt and p53 activation as well as p21 up-regulation induced by H_2O_2 is dependent on the ATM protein kinase. Caffeine is known to disrupt ATM-dependent responses likely through direct inhibition of ATM kinase activity (20), and KU-55933 is a specific and potent inhibitor of ATM kinase (21). Both inhibitors inhibited H_2O_2-induced ATM (Ser^{1981}), Akt (Ser^{473}), and p53 (Ser^{15}) phosphorylation (*lanes 3–5* in Fig. 2, *B* and *C*), in addition to p21 induction (*lanes 6–8* and *lanes 11–13* in Fig. 2*D*). Thus, ATM kinase played a major role in transducing H_2O_2-induced DNA damage signaling in HUVECs. Because an Akt/p53/p21-dependent pathway has been reported in endothelial cells (6), ATM thus likely regulates the cellular response to oxidative stress via phosphorylation of Akt and p53 then induction of p21 in sequence. Furthermore, NAC or KU-55933 also

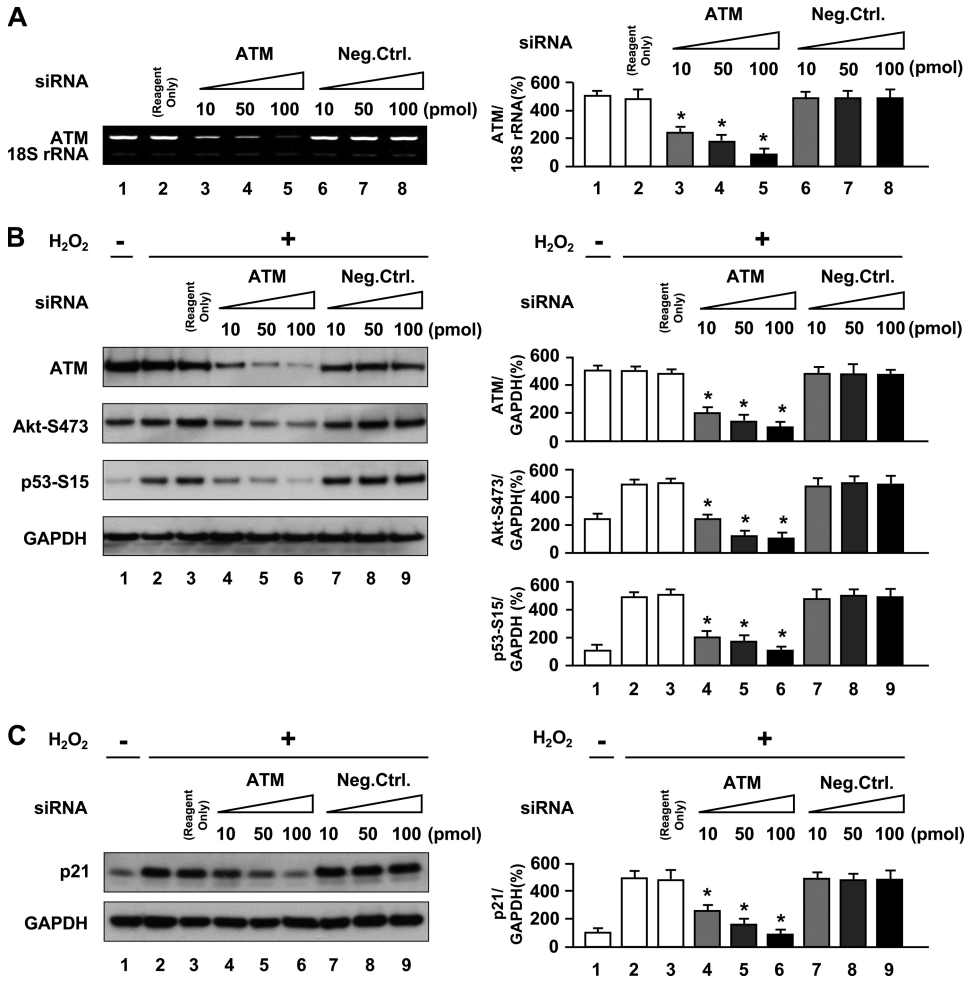

FIGURE 4. **Knockdown of ATM by ATM siRNA inhibits oxidative stress-induced activation of Akt and p53 and induction of p21 expression.** *A*, effect of siRNA against ATM on expression of ATM as analyzed by RT-PCR. *B* and *C*, Western blot analysis of the effects of siRNA against ATM on expression of total ATM, Akt phosphorylation (Ser^{473}), p53 phosphorylation (Ser^{15}), and p21 induction. Cells were transfected with siRNA against ATM for 72 h followed by incubation with 100 μM H_2O_2 for 30 min in *B* or 3 h in *C*. GAPDH was used as loading control. Values are mean ± S.E. (*error bars*) ($n = 3$). *, $p < 0.05$ *versus* cells transfected with the same concentration of negative control siRNA. Representative blots are shown in the *left panels* whereas corresponding quantitations are shown in the *right panels*. *Reagent Only*, cells transfected with Lipofectamine 2000 alone.

greatly reduced phosphorylated ATM nuclear fluorescence and foci formation (Fig. 3*A*). Collectively, H_2O_2 induced DNA damage and stimulated autophosphorylation of ATM in addition to formation of discrete nuclear foci together with subsequent induction of phosphorylation of Akt, p53, and up-regulation of p21 expression in an ATM-dependent manner.

Because the DNA damage response pathway triggers senescence (22) and because p53 and p21 were described to be major players in the induction of senescence (23, 24), we next addressed the functional effects of activation of the ATM/Akt/p53/p21 pathway on endothelial cells, namely in the form of induction of senescence which is a consequence of endothelial dysfunction. We induced premature endothelial senescence by addition of H_2O_2 to 100 μM as shown by SA-β-gal assay, a recognized surrogate index of senescent cells (25). We found that percentage of HUVECs positive for SA-β-gal was markedly increased in cells treated with H_2O_2, compared with cells incubated without H_2O_2 treatment (*panel 2* in Fig. 3*B* and *lane 2* in Fig. 3*C*). Furthermore, pretreatment with NAC, caffeine, or KU-55933 resulted in significant reduction of senescent (SA-β-gal-positive) cells compared with those exposed to H_2O_2 alone (Fig. 3, *B* and *C*). Thus, activation of ATM by H_2O_2 promotes endothelial cell senescence and contributes to vascular pathogenesis.

Abrogation of ATM Blocks Effects of Oxidative Stress on Endothelial Cells—We further examined the requirement of ATM expression in H_2O_2-induced premature senescence by abrogating ATM in cells using RNA interference. Knockdown of ATM in HUVECs by siRNA reduced ATM mRNA and protein levels (Fig. 4, *A* and *B*). Cells transfected with ATM siRNA showed reduced ATM expression with inhibition of Akt and p53 phosphorylation (*lanes 4–6* in Fig. 4*B*) in addition to down-regulation of p21 expression (*lanes 4–6* in Fig. 4*C*). As expected, ATM nuclear fluorescence was also markedly decreased in cells with ATM knocked down (Fig. 5*A*). Furthermore, knockdown of ATM by siRNA suppressed increase in SA-β-gal-positive cells induced by H_2O_2 (*panels 5* and *6* in Fig. 5*B* and *lanes 5* and *6* in Fig. 5*C*), which were comparable with the changes seen when HUVECs were treated with antioxidant or ATM inhibitor. Moreover, down-regulation of Akt, p53, or p21 by siRNA also suppressed an increase in SA-β-gal-positive cells induced by H_2O_2 (supplemental Figs. 4 and 5). Thus, RNA interference experiments further confirmed that ATM and its downstream molecules, Akt, p53, and p21, mediate actions of oxidative stress on endothelial cells to induce senescence.

Abrogation of Senescent Phenotype in Aorta of ATM Knock-out Mice—To test whether ATM mediates vascular endothelial cell senescence *in vivo*, we administered STZ to ATM knock-out mice and wild-type littermates to induce hyperglycemia-induced endothelial dysfunction because vascular endothelial cell senescence has been previously documented to be induced in STZ-diabetic mice (26). Western blot analysis for ATM protein levels in the thoracic aortas of heterozygous knock-out mice showed marked reductions to levels almost comparable with those of homozygote knock-out mice in contrast to robust levels as seen in wild-type mice (Fig. 6*B* and supplemental Fig. 7*A*) although the mechanisms of reduced protein levels in heterozygous knock-out mice are unclear. STZ-treated mice showed an elevation in blood glucose levels compared with STZ-untreated mice (*lanes 2*, *4*, and *6* in Fig. 6*C*). SA-β-

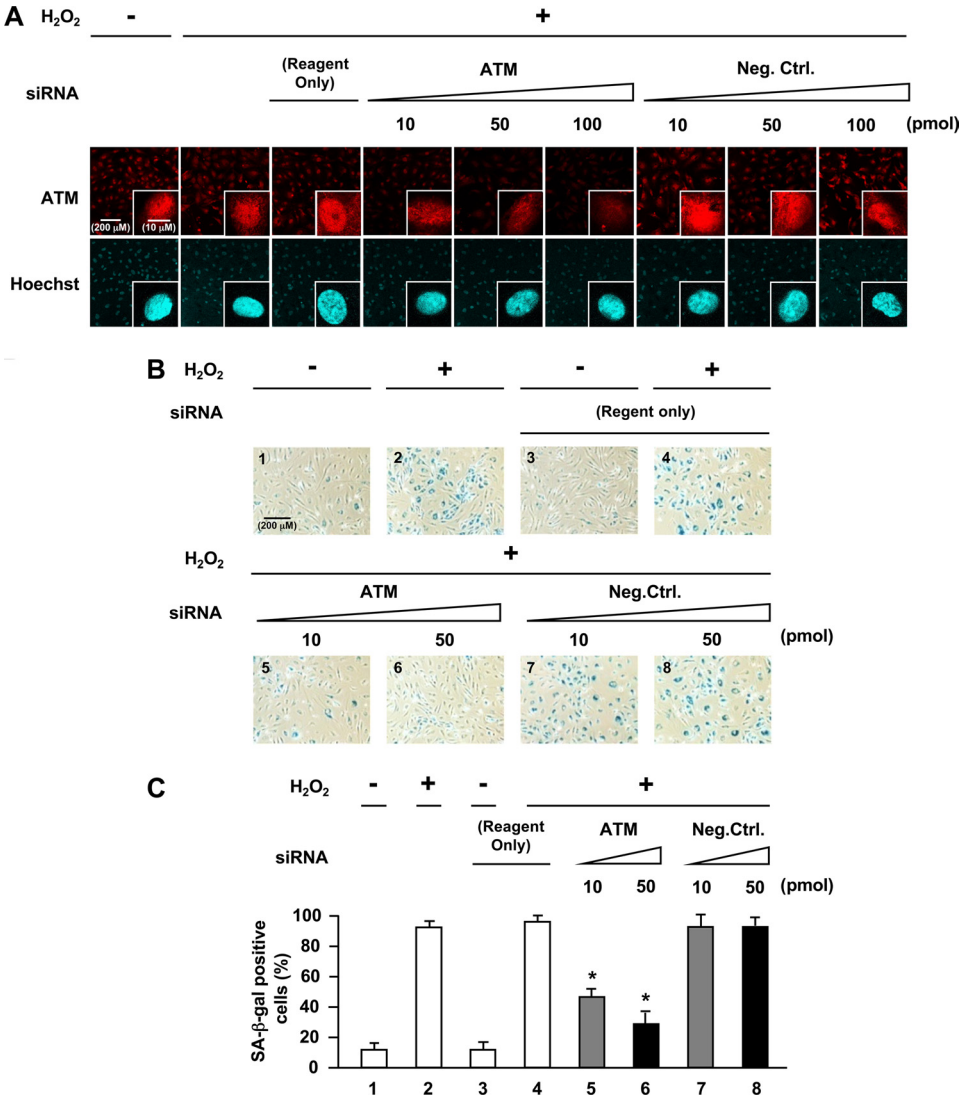

FIGURE 5. **Effects of abrogation of ATM expression by siRNA against ATM in oxidative stress-induced endothelial senescence.** *A*, immunofluorescence analysis of the effect of siRNA against ATM on total ATM. Transfected cells were immunostained for total ATM. Hoechst 33258 was used as nuclear stain (*blue*). Original magnification, ×200 and ×630. *Scale bar*, 200 μm and 10 μm, respectively. ATM nuclear fluorescence was greatly decreased in ATM knock-down cells. *B*, staining of SA-β-gal activity in ATM knock-down cells. *C*, quantification of percentage of SA-β-gal-positive cells in ATM knock-down cells. Values are mean ± S.E. (*error bars*) ($n = 3$). *, $p < 0.05$ *versus* cells transfected with the same concentration of negative control siRNA (*lane 7* or *lane 8*, respectively) ($n = 3$ each). Original magnification, ×100. *Scale bar*, 200 μm. *Reagent Only*, cells transfected with Lipofectamine 2000 alone. Knockdown of ATM by siRNA suppressed the increase in SA-β-gal-positive cells induced by H_2O_2.

gal activity was observed in the thoracic aortas of STZ-diabetic wild-type mice but not in STZ-diabetic ATM knock-out mice (Fig. 6, *D* and *E*). Cross-sections of thoracic aortas stained with SA-β-gal showed that positive areas were mostly localized to the luminal surface (Fig. 6*F*) which also stained positive for von Willebrand factor, indicating localization to vascular endothelial cells and not the extracellular matrix compared with normal rabbit IgG antibody (Fig. 6*G* and supplemental Fig. 6*A*). p21 and p16 are cyclin-dependent kinase inhibitor genes that are used as senescence markers. SA-β-gal-positive areas of cross-sections of thoracic aortas stained positive for p21 and p16 (Fig. 6*H* and 6*I*) but not for normal mouse IgG antibody used as a negative control (supplemental Fig. 6*B*). These results indicate that ATM is important for the induction of endothelial cell senescence in aortas of STZ-diabetic mice, which is consistent with *in vitro* cellular experiments.

DISCUSSION

Oxidative stress caused by reactive oxygen species plays an important causal role in senescence and age-related vascular diseases, including atherosclerosis and diabetic vasculopathy (7, 27, 28). Despite the wealth of knowledge on the effects and actions of oxidative stress on endothelial cells, characterization of involved regulatory pathways allowing for targeted molecular intervention with therapeutic intent had remained elusive.

We showed that ATM is involved in oxidative stress-induced endothelial dysfunction and premature senescencethroughanAkt/p53/p21-dependent pathway. Cellular experiments using HUVECs showed that the ATM/Akt/p53/p21 pathway was involved in oxidative stress-induced cellular senescence *in vitro*. Experiments using antioxidant and specific ATM inhibitory compounds or siRNA against ATM inhibited oxidative stress-induced cellular senescence thus confirming involvement of ATM and its dependent pathway. Furthermore, ATM induced endothelial cellular senescence *in vivo* in the aorta of diabetic wild-type mice but not in ATM knock-out mice. STZ-diabetic $ATM^{+/-}$ mice exhibit reduction in SA-β-gal-positive cells to levels almost comparable with those seen in STZ-diabetic $ATM^{-/-}$ mice. Reduction of ATM protein expression in heterozygote knock-out mice may account for the difference seen in endothelial senescence between wild-type and heterozygous knock-out mice. Collectively, the findings presented here indicate the importance of ATM in the induction of endothelial cell senescence induced by oxidative stress and abrogation of ATM resulting in a dysregulated response to pathophysiological stress in cardiovascular endothelial cells.

We further showed that ATM lies upstream from the Akt/p53/p21 pathway and that oxidative stress as sensed through ATM possibly in response to oxidative DNA damage is the initiating "trigger" and plays an instructive role in activation of this signaling pathway. Previous studies also demonstrated that ATM is a major upstream activator of Akt through control of

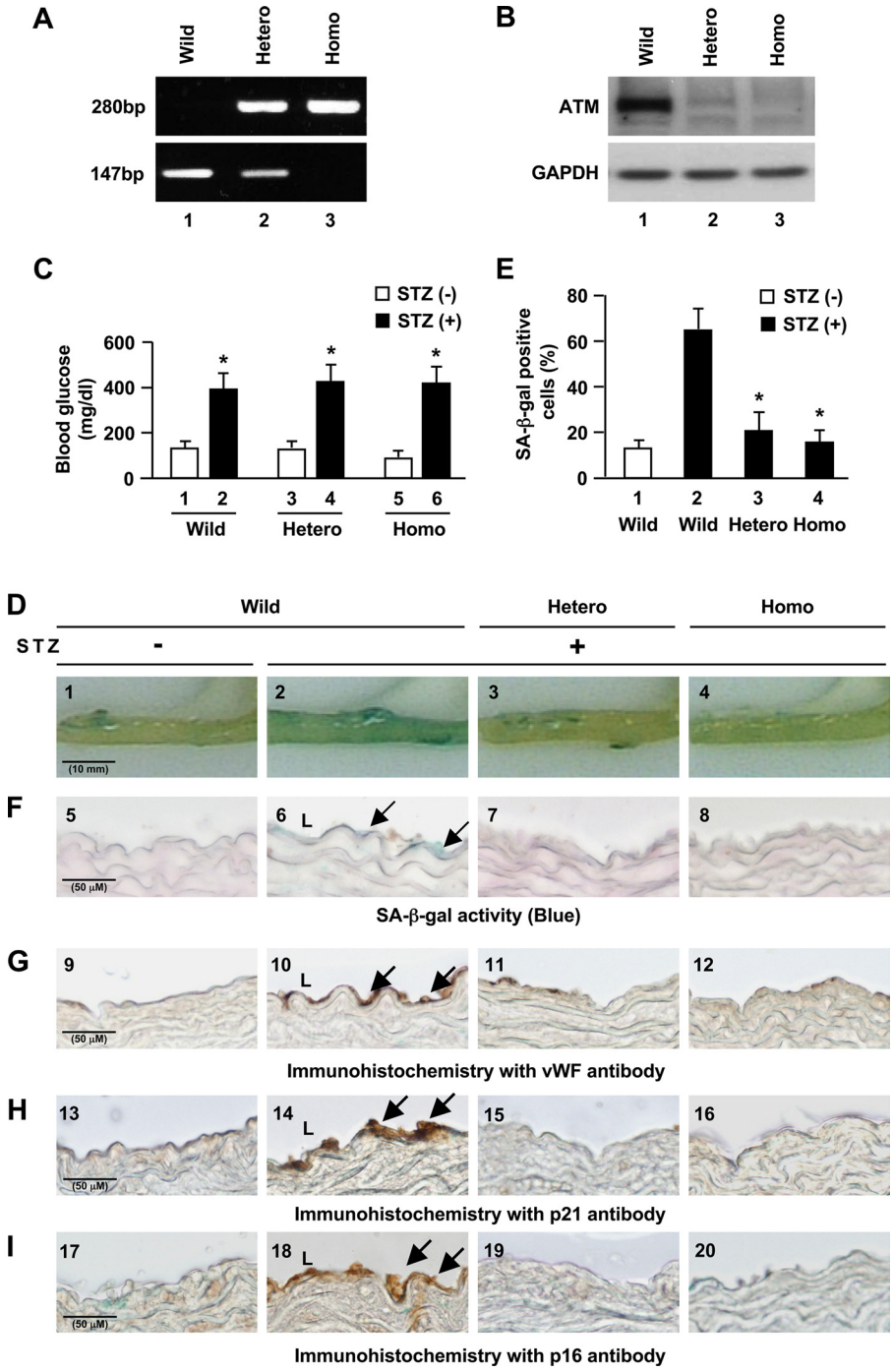

FIGURE 6. **Senescent endothelial cells in aortas of STZ-diabetic ATM knock-out mice.** Six respective $ATM^{+/+}$ (*Wild*), $ATM^{+/-}$ (*Hetero*), and $ATM^{-/-}$ (*Homo*) mice were used. *A*, genotyping analysis for ATM mice. *B*, Western blot analysis of ATM expression in the thoracic aortas. *C*, blood glucose levels measured before and after treatment with STZ. Values are mean ± S.E. (*error bars*). *, $p < 0.05$ *versus* STZ (−) mice (*lane 1*, *lane 3*, or *lane 5*, respectively). *D*, SA-β-gal activity (*blue*) in the thoracic aortas from mice at 10 days after treatment with STZ. *E*, quantitation of percentage of SA-β-gal-positive cells in the STZ-treated thoracic aortic samples. Values are mean ± S.E. *, $p < 0.05$ *versus* STZ (+) mice. *F*, sections of SA-β-gal stained thoracic aortas. *Arrows* indicate SA-β-gal-positive cells mostly localized to the luminal surface in the cross-section of the thoracic aortas. *G*, immunohistochemistry for von Willebrand factor, an endothelial cell marker, in the thoracic aortas (*brown*). *Arrows* indicate positive staining in the endothelium. *H* and *I*, immunohistochemical staining of p21 and p16 (*brown*). *Scale bar*, 50 μm and 10 mm, respectively.

Ser^{473} phosphorylation in response to insulin or ionizing radiation, which results in radiosensitivity or resistance to insulin in cell lines derived from A-T patients and ATM knock-out mice (15) or in muscle cells (29). However, in vascular endothelial cells stimulated by oxidative stress, we demonstrated for the first time to our knowledge that ATM regulates endothelial senescence through activation of Akt. Further, the pathway downstream of Akt through p53 and p21 has been well studied as a central pathophysiological signaling pathway in endothelial cells, especially in response to insulin (6, 7). However, whether the Akt/p53/p21 pathway is also activated by oxidative stress has not been clear. Our results thus indicate that this pathway is activated by oxidative damage and most importantly, regulated by ATM. γ-H2AX and 53BP1 foci formation was induced by oxidative stress, thus further providing supportive evidence that the oxidative stress-induced ATM-Akt/p53/p21 pathway is activated by DNA DSBs (supplemental Fig. 3).

Although the DNA damage response has been pursued mainly in oncogenesis and cancer-related fields and recently in regulation of senescence (1–3), as ATM has been shown to be activated by oxidative stress in hematopoietic cells (8), it is not beyond reason and in fact quite reasonable that ATM and the DNA damage response are involved in the vasculature as a response to oxidative stress albeit unexpected and unappreciated. Previous studies by ourselves initially suggested that the DNA damage response is activated in cardiovascular pathogenesis through the action of poly(ADP-ribose)polymerase-1 (PARP-1) (30), but identification and characterization of the actions of the central signaling molecule, ATM, in cardiovascular regulation provides further compelling evidence for the importance of this pathway in regulation of the vasculature and its diseases.

Our findings might explain in part the underlying mechanisms of the congenital disease condition of A-T in which the ATM gene is mutated. One of the hallmark characteristic phenotypes of A-T is vascular dysplasia and dysfunction, which pronounces as telangiectasia. Pathologically, vascular degeneration as characterized by loss of elastic fibers and proliferation of smooth muscle cells is seen. Patients that sur-

vive to later years are also known to be prone to ischemic heart disease (31). Although the precise underlying mechanism for the latter is unknown, in general, progression of coronary artery disease involves accelerated atherosclerosis in which oxidative stress of the endothelium and related cells plays a major contributory role. Response to oxidative stress in the vasculature may be disrupted in A-T patients. Dysregulation of endothelial cell function might lead to pathophysiological states such as vascular dysfunction in developmental states and accelerated atherosclerosis in adults. Better understanding the cellular response to oxidative stress with a focus on ATM is expected to shed further light on the pathogenesis of A-T and to clarify alternative pathological pathways that are activated in response to oxidative stress when deficient for ATM as well as to provide new insight into the molecular mechanisms underlying age-related cardiovascular pathologies such as atherosclerosis in which ATM might pose a new therapeutic target for vascular pathologies involving oxidative stress.

In conclusion, we show that oxidative stress can induce cellular senescence in HUVECs as shown by staining for SA-β-gal, which was associated with an ATM-dependent Akt/p53/p21 signaling pathway. Our findings might in part explain underlying mechanisms of the pathogenesis of the disease ataxia telangiectasia in which vascular dysplasia and dysfunction are seen, as well as suggesting that ATM may be a new therapeutic target for cardiovascular pathologies.

REFERENCES

1. Bartkova, J., Rezaei, N., Liontos, M., Karakaidos, P., Kletsas, D., Issaeva, N., Vassiliou, L. V., Kolettas, E., Niforou, K., Zoumpourlis, V. C., Takaoka, M., Nakagawa, H., Tort, F., Fugger, K., Johansson, F., Sehested, M., Andersen, C. L., Dyrskjot, L., Ørntoft, T., Lukas, J., Kittas, C., Helleday, T., Halazonetis, T. D., Bartek, J., and Gorgoulis, V. G. (2006) *Nature* **444,** 633–637
2. Bartkova, J., Horejsí, Z., Koed, K., Krämer, A., Tort, F., Zieger, K., Guldberg, P., Sehested, M., Nesland, J. M., Lukas, C., Ørntoft, T., Lukas, J., and Bartek, J. (2005) *Nature* **434,** 864–870
3. Gorgoulis, V. G., Vassiliou, L. V., Karakaidos, P., Zacharatos, P., Kotsinas, A., Liloglou, T., Venere, M., Ditullio, R. A., Jr., Kastrinakis, N. G., Levy, B., Kletsas, D., Yoneta, A., Herlyn, M., Kittas, C., and Halazonetis, T. D. (2005) *Nature* **434,** 907–913
4. Zeiher, A. M., Drexler, H., Saurbier, B., and Just, H. (1993) *J. Clin. Invest.* **92,** 652–662
5. Breitschopf, K., Zeiher, A. M., and Dimmeler, S. (2001) *FEBS Lett.* **493,** 21–25
6. Miyauchi, H., Minamino, T., Tateno, K., Kunieda, T., Toko, H., and Komuro, I. (2004) *EMBO J.* **23,** 212–220
7. Minamino, T., and Komuro, I. (2007) *Circ. Res.* **100,** 15–26
8. Ito, K., Hirao, A., Arai, F., Matsuoka, S., Takubo, K., Hamaguchi, I., Nomiyama, K., Hosokawa, K., Sakurada, K., Nakagata, N., Ikeda, Y., Mak, T. W., and Suda, T. (2004) *Nature* **431,** 997–1002
9. Barzilai, A., Rotman, G., and Shiloh, Y. (2002) *DNA Repair* **1,** 3–25
10. Shiloh, Y. (2003) *Nat. Rev. Cancer* **3,** 155–168
11. Ota, H., Eto, M., Kano, M. R., Ogawa, S., Iijima, K., Akishita, M., and Ouchi, Y. (2008) *Arterioscler. Thromb. Vasc. Biol.* **28,** 1634–1639
12. Bakkenist, C. J., and Kastan, M. B. (2003) *Nature* **421,** 499–506
13. Kozlov, S. V., Graham, M. E., Peng, C., Chen, P., Robinson, P. J., and Lavin, M. F. (2006) *EMBO J.* **25,** 3504–3514
14. Dupré, A., Boyer-Chatenet, L., and Gautier, J. (2006) *Nat. Struct. Mol. Biol.* **13,** 451–457
15. Viniegra, J. G., Martínez, N., Modirassari, P., Losa, J. H., Parada Cobo, C., Lobo, V. J., Luquero, C. I., Alvarez-Vallina, L., Ramón y Cajal, S., Rojas, J. M., and Sánchez-Prieto, R. (2005) *J. Biol. Chem.* **280,** 4029–4036
16. Lavin, M. F. (2008) *Nat. Rev. Mol. Cell Biol.* **9,** 759–769
17. Bencokova, Z., Kaufmann, M. R., Pires, I. M., Lecane, P. S., Giaccia, A. J., and Hammond, E. M. (2009) *Mol. Cell. Biol.* **29,** 526–537
18. Rappold, I., Iwabuchi, K., Date, T., and Chen, J. (2001) *J. Cell Biol.* **153,** 613–620
19. Zafarullah, M., Li, W. Q., Sylvester, J., and Ahmad, M. (2003) *Cell. Mol. Life Sci.* **60,** 6–20
20. Zhou, B. B., Chaturvedi, P., Spring, K., Scott, S. P., Johanson, R. A., Mishra, R., Mattern, M. R., Winkler, J. D., and Khanna, K. K. (2000) *J. Biol. Chem.* **275,** 10342–10348
21. Hickson, I., Zhao, Y., Richardson, C. J., Green, S. J., Martin, N. M., Orr, A. I., Reaper, P. M., Jackson, S. P., Curtin, N. J., and Smith, G. C. (2004) *Cancer Res.* **64,** 9152–9159
22. von Zglinicki, T., Saretzki, G., Ladhoff, J., d'Adda di Fagagna, F., and Jackson, S. P. (2005) *Mech. Ageing Dev.* **126,** 111–117
23. Brown, J. P., Wei, W., and Sedivy, J. M. (1997) *Science* **277,** 831–834
24. Kang, J. Y., Kim, J. J., Jang, S. Y., and Bae, Y. S. (2009) *Mol. Cells* **28,** 489–494
25. Dimri, G. P., Lee, X., Basile, G., Acosta, M., Scott, G., Roskelley, C., Medrano, E. E., Linskens, M., Rubelj, I., Pereira-Smith, O., Peacocke, M., and Campisi, J. (1995) *Proc. Natl. Acad. Sci. U.S.A.* **92,** 9363–9367
26. Yokoi, T., Fukuo, K., Yasuda, O., Hotta, M., Miyazaki, J., Takemura, Y., Kawamoto, H., Ichijo, H., and Ogihara, T. (2006) *Diabetes* **55,** 1660–1665
27. Finkel, T., and Holbrook, N. J. (2000) *Nature* **408,** 239–247
28. Davies, K. J. (2000) *IUBMB Life* **50,** 279–289
29. Halaby, M. J., Hibma, J. C., He, J., and Yang, D. Q. (2008) *Cell. Signal.* **20,** 1555–1563
30. Suzuki, T., Nishi, T., Nagino, T., Sasaki, K., Aizawa, K., Kada, N., Sawaki, D., Munemasa, Y., Matsumura, T., Muto, S., Sata, M., Miyagawa, K., Horikoshi, M., and Nagai, R. (2007) *J. Biol. Chem.* **282,** 9895–9901
31. Swift, M., and Chase, C. (1983) *Lancet* **1,** 1049–1050 .